

LISA: BEAM TRANSPORT AND DYNAMICS

S. Bartalucci, M. Bassetti, C. Biscari, S. Kulinski*, L. Palumbo^o, P. Patteri, M. Preger, C. Sanelli, B. Spataro, F. Tazzioli, F. Tian^{oo} and J. Xu^{oo}

INFN, Laboratori Nazionali di Frascati, C.P.13, 00044 Frascati, Italy
 *On leave of absence from Institute for Nuclear Studies, Swierk, Poland
^oDip. Energetica Univ. Roma 'La Sapienza', V. A. Scarpa 14, 00161 Roma, Italy
^{oo}On leave of absence from I.H.E.P., P.O. BOX 918, Beijing, P.R.China

Abstract

The 1.1 MeV electron beam injected into the superconducting (SC) Linac is accelerated to 25 MeV; after the extraction it can follow two alternative paths: either through the undulator and then back to the Linac entrance for energy recovery, or through the recirculation arc into the Linac to be further accelerated to 49 MeV and used to generate shorter wavelength radiation in the FEL. The recirculation arcs have been designed taking into account the optical requirements for the FEL cavity and for the insertion of an Optical Klystron and of a phase adjusting system. Beam dynamics inside the cavities, including beam stability problems in the SC Linac, have been studied.

Introduction

LISA¹, in construction at Frascati INFN Laboratories, is a test-bench machine aimed at studying the acceleration techniques with SC cavities; its beam will be used in a high efficiency FEL experiment in the infrared wavelength region. LISA will allow to study also low emittance electron guns, beam recirculation and beam break-up problems.

The accelerator consists of a SC Linac and a recirculating arc which can be used both for energy doubling and for energy recovery after interacting with a FEL. A sketch of the accelerator layout is shown in fig. 1.

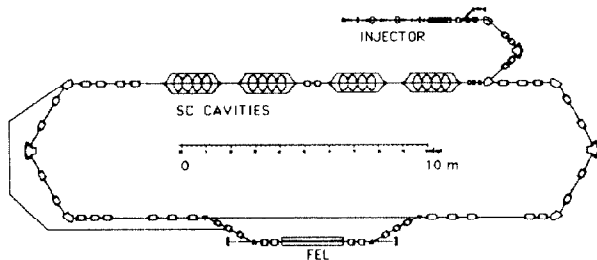


Fig. 1 - Sketch of LISA layout.

Lattice description

The Linac is composed by four SC cavities, useful length 1.2 m, each one containing 4 π -mode cells working at $f = 500$ MHz. A sketch of the cavity geometry is shown in fig. 2.

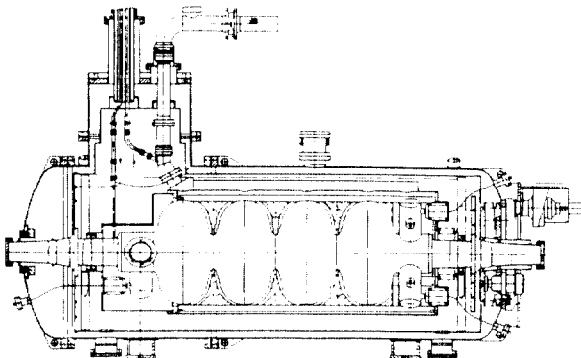


Fig. 2 - LISA SC cavity.

Each cavity is inserted in a cryostat, and a quadrupole doublet between the second and the third cryostat is used for transverse focusing. The quadrupoles are 10 cm long and the maximum gradient is 0.5 T/m. The nominal average accelerating gradient is 5 MV/m, giving therefore a final energy of 25 MeV in the first passage and 49 MeV in the second one. The possibility of energy recovering after the interaction with FEL @ 25 MeV is also envisaged to increase the FEL efficiency.

General description of the arc.

The transport line from the SC Linac to the FEL undulator fulfils two basic conditions: the achromaticity and the isochronism. The easier solution for a symmetric π -bend with these characteristics are three bending magnets of $\pi/3$ bend with quadrupoles symmetrically arranged which force the dispersion function D to the symmetry around the center of the arc (achromatism) and to the isochronism condition:

$$\int D/\rho ds = 0 \quad (1)$$

(ρ is the curvature radius in the dipoles). The D value in the central bending magnet must then be negative and a strong horizontal focusing is needed to obtain it. The bendings are sector magnets; the betatron functions have been forced to the symmetry with respect to the center of the arc.

The beam is transported to the undulator through a chicane on the horizontal plane. The difference in path length between the chicane and the direct path necessary for energy doubling must be an odd multiple of half rf wavelength ($\lambda/2 = 0.3$ m), because of the relative beam-rf phase requirements. This imposes a condition on the length of the chicane according to the bending angle α and the curvature radius ρ . Being L the distance between the two chicane rectangular dipoles:

$$L + 2\rho\alpha = 2\rho\sin\alpha + L\cos\alpha + n\lambda/4 \quad n \text{ odd} \quad (2)$$

$L \sim 3$ m, and $\alpha=30^\circ$ ($n=3$) have been chosen. The chicane contains two focusing quadrupoles and a defocusing one around the point where the dispersion passes through zero, i.e. where its contribution is felt only on the vertical plane. The small contribution from the chicane to the integral (1) is compensated changing accordingly the dispersion in the arc.

The matching section from the exit of the last Linac cell to the arc entrance is 4.5 m long and contains four quadrupoles. Its tunability has been tested for input values of both transverse betatron functions varying between 5 and 30 m and values of α between -2 and +2, showing a wide flexibility.

The second matching section, 5.4 m long, from the arc to the chicane contains six quadrupoles and has been designed with a free length of 1.2 m to be utilized for an Optical Klystron.

The last section from the chicane to the undulator contains two quadrupoles, which together with the central quadrupole of the chicane adjust the betatron functions to the undulator.

When the accelerator will work on the doubling energy configuration the beam will pass straight instead of going through the chicane. The second matching section can match the beam also to pass through the free section, 12 m long, opposite to the Linac, just opportunely tuning the quadrupole gradients.

The optical functions all along the arc are plotted in figs. 3a, 3b for the energy recovery (or passage through FEL @ 25 MeV) and energy doubling configurations respectively.

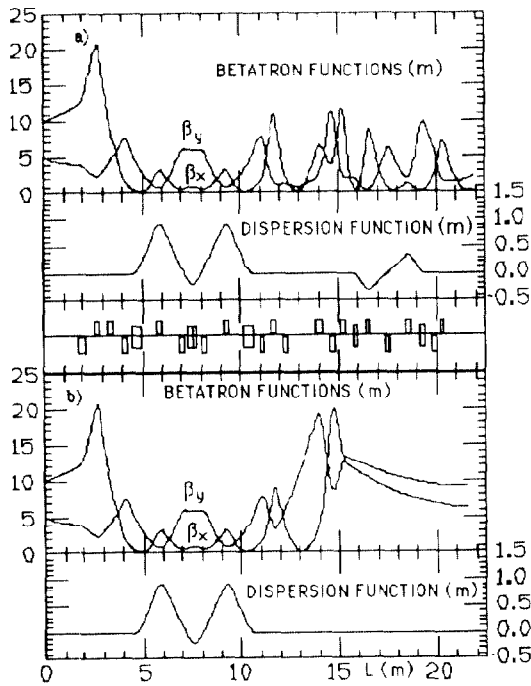


Fig. 3 - Optical functions from the SC Linac to the center of FEL undulator (a) and along half recirculation arc (b).

Fields in the cavities

An extensive calculation of monopole and dipole oscillating modes in the SC cavity has been performed by means of the codes URMEL and OSCAR-2D2. The on-axis distribution of the longitudinal electric field E_z has been used to study the beam dynamics under the fields of the accelerating TM_{010} π mode. This is of utmost importance in the case of LISA, since the presence of the end tubes changes the field profile considerably and this in turn influences the beam dynamics and notably that of non-relativistic particles.

E_z was developed in Fourier series along the accelerating cells and in the end tube zone where it is extended, i. e. from $z = -L/2$ to $z = L/2$ with $L = 1.35$ m, obtaining the analytical expression which makes particle tracking through the structure easier. The first 6 harmonics were retained with a rms error of 3%:

$$E_z \sim \sum_{n=1}^6 E_n \sin(k_n z) \sin(\omega t + \varphi)$$

being $k_n = 2n\pi/L$, $\omega = 2\pi f$ and φ the injection phase at $z = -L/2$. The computed field profile together with the six harmonics is shown in fig. 4. The E_z and H_0 field components were derived from the E_z expression according to Maxwell's equations, assuming a radial dependence $\propto J_0(k_r r)$ for E_z .

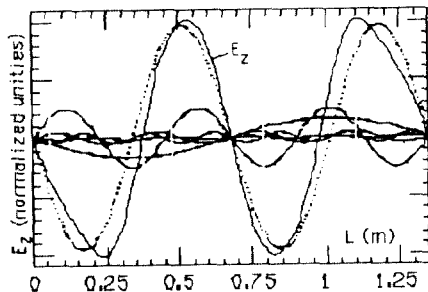


Fig. 4 - E_z profile and 6 harmonics.

Beam dynamics in cavities

A numerical analysis of the longitudinal and transverse dynamics in the vicinity of the rf cavity axis has been worked out considering the fields described above. The equations of motion are written in terms of position (r, z) and momentum (p_r, p_z) for an infinitesimal time step; then the relevant dynamical quantities are propagated through the whole cavity using the matrix formalism:

$$p_z(t+dt) = p_z(t) + e E_z(z,t) dt$$

$$\begin{pmatrix} r \\ p_r \end{pmatrix}_{(t+dt)} = \begin{pmatrix} 1 & \frac{c \beta_z dt}{p_r} \\ \frac{e(1+\beta_z^2)}{2} \frac{\partial E_z}{\partial z} dt & 1 \end{pmatrix} \begin{pmatrix} r \\ p_r \end{pmatrix}_{(t)} \quad (1)$$

where β_z is the longitudinal relativistic factor. In fig. 5 the accelerating field seen by a particle entering the first cavity with different phase shifts φ (180° apart) is shown. The interrupted curves correspond to particles which, being decelerated, lose their energy. The maximum energy gain is obtained for those particles which meet a low decelerating field in the end-tubes but are fully accelerated in the 4-cell structure.

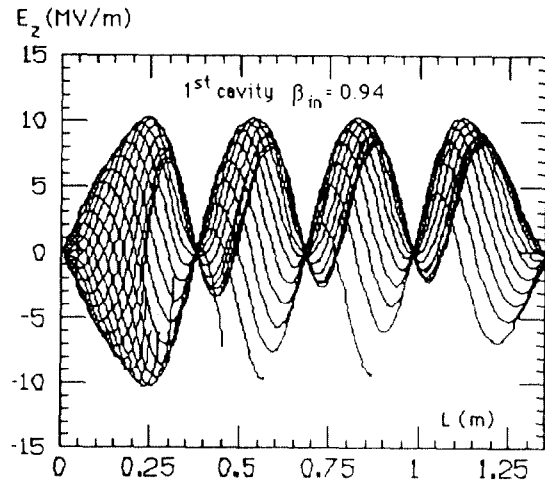


Fig. 5 - E_z as seen by particles with different injection phases.

The optimum injection phase is $\varphi_{opt} = 126^\circ$ in the first cavity where $\beta_{in} = 0.94$, while in the other three cavities ($\beta_{in} = 1$) $\varphi_{opt} = 135^\circ$, as it is shown in fig. 6.

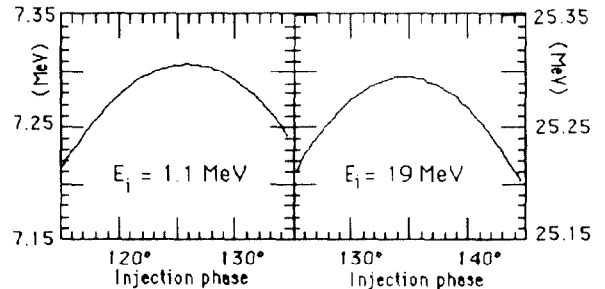


Fig. 6 - Final energy versus injection phase in first and last cavities.

The induced energy spread depends both on the bunch length and on the injection phase as shown in fig. 7 for the first and last cavity: the dependence on bunch length is more peaked for $\beta_{in}=1$. For the nominal value (bunch length $\sim 1.5^\circ$) the induced energy spread is very small: 0.8 keV in the first cavity and 0.7 keV in the other three if $\varphi = \varphi_{opt}$; if the bunch length were longer being this energy spread correlated with the position along the bunch, it could be compensated choosing alternatively injection phases on the right and on the left of φ_{opt} for the different cavities.

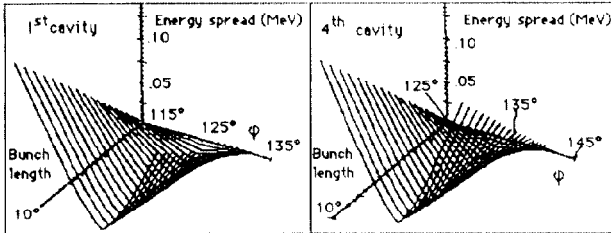


Fig. 7 - Induced energy spread versus injection phase and bunch length

However, analysis of the transverse dynamics shows that particles injected with φ_{opt} are just on the border of "stable" and "unstable" trajectories.

Fig. 8 shows the trajectories (r, z) of 20 particles chosen on a phase space ellipse (r, r') (with Twiss parameters $\alpha = 0.$, $\beta = 5$ m and emittance 10π mm mrad), for three cases ($\varphi = 121^\circ, 126^\circ, 131^\circ$), transmitted through the first cavity; it is clear that the injection phase plays a relevant role on the transverse stability.

The trace of the matrix R propagating (r, p_r) along the cavity and obtained as the product of the infinitesimal matrices above defined is plotted in fig. 9 versus the longitudinal z-coordinate for the first and the last cavity, varying the phase φ of $\pm 5^\circ$ from φ_{opt} . The stability requirement $|\text{tr}(R)| < 2$ is fulfilled for $\varphi > \varphi_{opt}$. There is a strong dependence on the ratio between the energy gain per cavity and the input energy; in fact as this ratio decreases the effect of the cavity on the transverse plane becomes weaker.

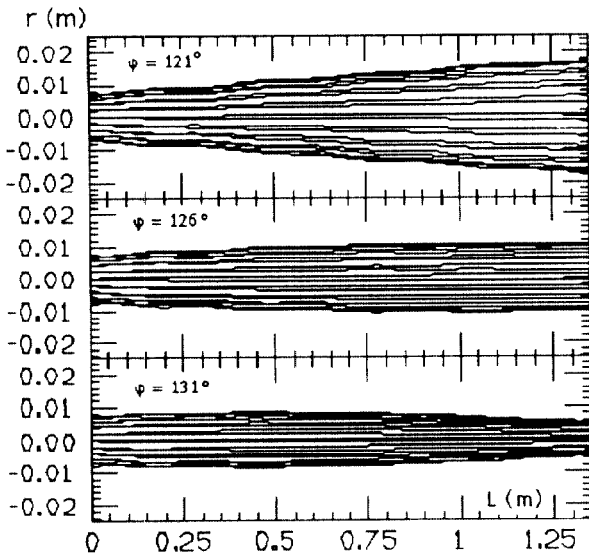


Fig. 8 - Evolution of r along the 1st cavity for three different injection phases.

The rf field acts as a focusing ($\varphi > \varphi_{opt}$) or defocusing ($\varphi < \varphi_{opt}$) lens, so that alternating the values of φ as explained above between adjacent cavities a FODO structure is obtained.

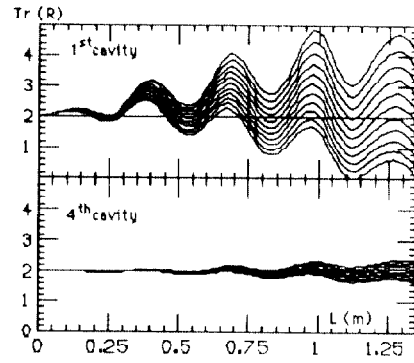


Fig. 9 - Trace of the transverse matrix for the first and the last cavity for particles with different injection phases

The transport matrix R, as it has unity determinant, can be represented as:

$$\begin{pmatrix} \cos\theta + \eta \sin\theta & \xi \sin\theta \\ -\frac{(1 + \eta^2)}{\xi} \sin\theta & \cos\theta - \eta \sin\theta \end{pmatrix}$$

with $\theta = \text{acos}(\text{Tr}(R)/2)$; $\eta = (r_{11} - r_{22})/(2 \sin\theta)$; $\xi = r_{12}/\sin\theta$. These parameters are affected by the real accelerating field distribution, by the relative energy gain $\Delta E/E_{in}$ per cell and by the relativistic factor β_z . They differ from the values derived with the analytical approach³ which considers only the first field harmonic and assumes the asymptotic condition of $\Delta E/E_{in} \ll 1$. The behaviour of the three parameters, normalized to those computed in ref. [3] is shown in figs.10, where we consider first the effect of low injection energy (a) and then the effect of the real field in the asymptotic case (b). $\Delta E = 6$ MeV per cavity has been assumed. In fig (a) only the fundamental harmonic (the second one) is taken into account, and the three normalized parameters approach to the unity as β_z increases and $\Delta E/E_{in}$ decreases. It is worth noting in (b) that the effect of the end tubes on the real field distribution affects these parameters notably.

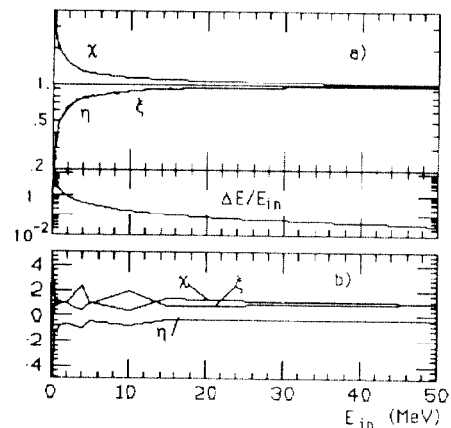


Fig. 10 - R matrix parameters: a) fundamental harmonic b) real field distribution.

References

- [1] F. Tazzioli et al.: "Status of the LISA superconducting Linac project", these Proceedings.
- [2] P. Fernandes, R. Parodi: "Computation of e.m. fields in TE and TM resonators and in wave guides", IEEE Trans. Magn. Mag-21(6) (1985) 2246.
- [3] E.E. Chambers: "Proceedings of the 1968 Summer Study on Superconducting Devices and Accelerators", BNL Report 50155, 1968.